

Efficient viscosity estimation from molecular dynamics simulation via momentum impulse relaxation

Gaurav Arya, Edward J. Maginn,^{a)} and Hsueh-Chia Chang

Department of Chemical Engineering, University of Notre Dame, Notre Dame, Indiana 46556

(Received 14 February 2000; accepted 11 May 2000)

A new momentum impulse relaxation method for obtaining the shear viscosity of Newtonian fluids using molecular dynamics simulations is introduced. The method involves the resolution of a decaying coarse-grain Gaussian velocity profile in a properly thermostated simulation box. This localized velocity profile, along with a modification of the periodic boundary conditions, allows computations in a periodic box with minimal phonon feedback due to periodicity. The short-time decay of the small-amplitude velocity profile yields shear viscosities for atomic and molecular species that are in quantitative agreement with those obtained using conventional techniques, but with more than an order of magnitude reduction in computational effort. © 2000 American Institute of Physics. [S0021-9606(00)51130-1]

I. INTRODUCTION

Several molecular dynamics methods have been developed over the years to estimate the macroscopic transport properties of fluids. The calculation of one of these properties, the shear viscosity, is of considerable practical interest. The molecular dynamics methods for calculating the shear viscosity fall into one of two main categories: equilibrium molecular dynamics (EMD) or nonequilibrium molecular dynamics (NEMD) techniques. The EMD techniques involve either the calculation of time correlation functions by measuring the decay of near-equilibrium fluctuations in properties of the fluid (Green–Kubo methods) or by accumulating displacements in properties over time (Einstein methods). The Green–Kubo relation^{1,2} for shear viscosity, η , is given by

$$\eta = \frac{V}{k_B T} \int_0^\infty \langle P_{xz}(0) P_{xz}(t) \rangle dt, \quad (1)$$

where $\langle \dots \rangle$ denotes the ensemble average, V is the volume, k_B is the Boltzmann's constant, T is the temperature, t is the time and P_{xz} is the xz component of the pressure tensor \mathbf{P} given by

$$\mathbf{P}V = \sum_{i=1}^N \frac{\mathbf{p}_i \mathbf{p}_i}{m_i} + \sum_{i=1}^N \sum_{j>i}^N \mathbf{r}_{ij} \mathbf{F}_{ij}, \quad (2)$$

where \mathbf{p}_i is the momentum vector for molecule i , $\mathbf{r}_{ij} = \mathbf{r}_i - \mathbf{r}_j$ is the vector joining the centers of molecules i and j , and \mathbf{F}_{ij} is the force between them. The above expression is known as the “molecular” virial, since the sum is over all the molecules, N . The shear viscosity can also be calculated from the “atomic” virial which is of similar form, except that the summation is over individual atomic species rather than molecules.

A weakness of both the EMD methods is that the shear viscosity suffers from substantial nonmonotonic system size

dependence.^{3,4} Another drawback is that the autocorrelation function in the Green–Kubo expression decays with long-time tails⁵ ($\sim t^{-3/2}$ as $t \rightarrow \infty$). Therefore, the integration in Eq. (1) when truncated at a finite $t = t_{\text{run}}$ contains truncation errors^{6,7} given by

$$\sigma = \left(\frac{2\tau}{t_{\text{run}}} \right)^{1/2}, \quad (3)$$

where σ is the uncertainty in the value of the viscosity, and τ is the relaxation time of the molecules. This means that prohibitively long EMD simulations have to be run for molecules with long relaxation times to achieve acceptable levels of error.

The NEMD techniques usually involve measuring the macroscopic steady-state response of the system to a perturbing field and relating the linear response to a transport coefficient. One of the earliest NEMD techniques, which maintains conventional periodic boundary conditions, involves imposing a spatially periodic external force on the molecules to generate an oscillatory velocity profile.⁸ The amplitude of this velocity profile at steady state is inversely related to the shear viscosity, and hence the viscosity can be calculated. The shear viscosity is wavelength dependent, however, and the Newtonian shear viscosity is obtained only in the long wavelength limit, i.e., in the limit $k \rightarrow 0$, where k is the wave vector of the oscillatory perturbation. This means that a very large simulation box is required to get reasonably accurate values of shear viscosity, which limits the usefulness of this technique. The reason for this box-size dependent viscosity is that the periodic boundary conditions allow acoustic modes (phonons) to propagate persistent fluctuations around the box due to periodic feedback.

The more successful NEMD techniques involve imposing a planar Couette flow velocity profile (i.e., zero wave vector techniques). One of the most efficient NEMD algorithms for shear viscosity is the Sllod algorithm.^{7,9} The Sllod algorithm has been used by several authors, and has been shown to be exact for arbitrarily large shear rates $\dot{\gamma}$, and is

^{a)}Electronic mail: ed@nd.edu

therefore appropriate for studying non-Newtonian regimes. The modified equations of motion for the Sllod algorithm are

$$\frac{d\mathbf{r}_i}{dt} = \frac{\mathbf{p}_i}{m_i} + \mathbf{r}_i \cdot \nabla \mathbf{u}, \quad (4)$$

$$\frac{d\mathbf{p}_i}{dt} = \mathbf{F}_i - \mathbf{p}_i \cdot \nabla \mathbf{u} - \alpha \mathbf{p}_i, \quad (5)$$

where \mathbf{F}_i is the force on molecule i , α is the thermostating multiplier, $\mathbf{u} = (u_x, 0, 0)$, and $u_x = \dot{\gamma} r_{iz}$, where z is the direction normal to the flow and x is the direction of flow. The Sllod algorithm is combined with the Lees–Edwards “sliding brick” periodic boundary conditions.¹⁰ The strain rate dependent shear viscosity is obtained from the constitutive equation

$$\eta(\dot{\gamma}) = \frac{-\langle P_{xz} \rangle}{\dot{\gamma}}. \quad (6)$$

The Newtonian shear viscosity is estimated by extrapolating the shear viscosities to zero shear rate. Both EMD and NEMD methods give similar values for the Newtonian shear viscosities, however, an advantage of this NEMD method is that the shear rate dependence of the viscosity is obtained directly from NEMD, while EMD provides the zero shear rate value only. One of the drawbacks of this NEMD method is that there is no generally accepted theoretical model for the shear rate dependence of the shear viscosity. The resulting Newtonian viscosity obtained from an NEMD simulation depends on the model used in the extrapolation procedure. To overcome this limitation, NEMD simulations at very small shear rates may be performed. However, this defeats the purpose of the NEMD method since these low shear rate simulations require nearly as much computation time as the EMD methods. Though the NEMD runs can be parallelized for different shear rates, the computational time required to obtain the viscosity is limited by these long simulation runs at low shear rates. Although refinements to the traditional NEMD methods are being developed which reduce the computational cost by improving the signal-to-noise ratio at small fields,^{11,12} viscosity calculation is still quite demanding.

In brief, the existing molecular dynamics (MD) methods for estimating the shear viscosity of fluids require long simulation times. For systems composed of big molecules, these simulations become prohibitively long, and therefore faster ways of obtaining the viscosity of fluids are required. In the present article, we present a novel technique for calculating Newtonian shear viscosities with significantly less computational effort than standard methods. This involves a short-time transient analysis of a Gaussian velocity impulse imposed on a periodic box at time $t=0$. A major obstacle in using periodic simulation boxes for both EMD and NEMD techniques is the anomalous phonon propagation of momentum through the periodic boundaries. We overcome this obstacle by using an initial coarse-grain velocity impulse much narrower than the box dimension. If the shear viscosity can be estimated from the short-time simulation before the relaxation reaches the box boundaries, phonon corruption can be

minimized. This is not possible with conventional NEMD methods, as steady equilibrium necessitates phonon equilibration across the periodic boundaries. To this end, we use a Gaussian profile whose relaxation is concentrated near its peak, away from the boundaries where phonon corruption dominates. We also modify periodic boundary conditions in the direction of momentum transport to better mimic a Gaussian decay in an infinite domain and to minimize periodic phonon feedback. We exploit the self-similarity of the Gaussian decay to anticipate the velocity modification at the boundary without explicit knowledge of the viscosity. As an application, this method is used to calculate the shear viscosity for argon and *n*-butane.

II. THEORY

Consider a parallel flow of a Newtonian fluid in the x direction in an infinite domain, with velocity $\mathbf{u}(y,t)$ expressed as $[u_x(y,t), 0, 0]$ in Cartesian coordinates. From a macroscopic hydrodynamic standpoint, neglecting effects of viscous heating, the transient motion of the fluid is determined by the Navier–Stokes equation, given by

$$\rho \left[\frac{\partial}{\partial t} + \mathbf{u} \cdot \nabla \right] \mathbf{u} = -\nabla P + \eta \nabla^2 \mathbf{u} + \rho \mathbf{g}, \quad (7)$$

where ρ is the density of the fluid, P is the pressure, η is the Newtonian shear viscosity, and \mathbf{g} is the external force per unit mass of the fluid. Assuming that the external force on the system is zero and that no pressure gradients exist in the system, Eq. (7) simplifies to the following equation in the x direction:

$$\frac{\partial u_x(y,t)}{\partial t} = \nu \frac{\partial^2 u_x(y,t)}{\partial y^2}, \quad (8)$$

where ν is the kinematic viscosity given by η/ρ . Let us impose the condition that at time $t=0$, $u_x(y,t)$ is described by the following Gaussian function:

$$u_x(y,0) = a_0 e^{-b_0 y^2}, \quad (9)$$

where parameters a_0 and b_0 are equal to the peak height, $u_p(0)$, and the inverse of the variance of the Gaussian function, $\sigma^{-2}(0)$, respectively. This then forms the initial condition for the partial differential equation given by Eq. (8).

In an infinite domain without specified length scales and wall dissipation, this velocity profile will decay with respect to time as a result of x -momentum transport along the y direction. The initial Gaussian profile decays in a self-similar manner such that the profile at every moment is a Gaussian

$$u_x(y,t) = \left[\frac{a_0^2}{(1+t/t_0)} \right]^{1/2} e^{-b_0 y^2 / (1+t/t_0)}, \quad (10)$$

where $t_0 = 1/4 \nu b_0$. In particular, the peak velocity, $u_p(t)$, which is equal to a_0 at time $t=0$, decays with respect to time as

$$u_p(t) = u_p(0) \left(1 + \frac{t}{t_0} \right)^{-1/2}. \quad (11)$$

Also, the variance of the profile, $\sigma^2(t)$, increases linearly with time as

$$\sigma^2(t) = \sigma^2(0) \left(1 + \frac{t}{t_0} \right). \quad (12)$$

Therefore, if $u_p(t)$ is plotted as a function of time and fitted to a function of the form $A/(1+Bt)^{1/2}$ (where A and B are equal to a_0 and $1/t_0$, respectively), the shear viscosity can be obtained from the relation

$$\eta = \frac{\rho B}{4b_0}. \quad (13)$$

Likewise, the shear viscosity could also be estimated by fitting the variance to a linear function in time. The essence of the algorithm presented here is to conduct a transient molecular dynamics simulation that satisfies the conditions outlined above. The Newtonian viscosity is then extracted from the decay of the Gaussian peak via Eq. (13).

III. SIMULATION ALGORITHM

This section describes the MD procedure adopted to simulate the above infinite system using a finite but periodic simulation box. We start with an equilibrated system of molecules in a simulation box centered at the origin, and of length L in the y direction. Standard periodic boundary conditions (PBC) are applied to the positions of all the molecules to model an infinite system, and the minimum image convention is maintained.

To initialize the Gaussian x -component velocity profile, the hydrodynamic velocity given by Eq. (9) is added to all the atoms of the molecules at $t=0$. For molecular systems, y is the center of mass of the molecule. A thermostat is used to keep the temperature at the desired value, where the temperature is specified in such a way so as to eliminate the contribution made from the mean kinetic energy of the molecules due to the drift velocity in the x direction. A system with a decaying velocity profile given by Eq. (10) conserves momentum in the y and z directions, but constantly loses the x -component of the momentum along the y direction. To model this transient behavior, we utilize standard PBC for the velocities in the x and z direction, but the velocity in the y direction is modified to incorporate this x -momentum ‘‘leak’’ through the top and bottom faces of the simulation box.

To see how this is done in practice, consider a molecule leaving the bottom face of the simulation box as shown in Fig. 1 (a two-dimensional box is shown here for simplicity). According to standard PBC, the image of this molecule would enter at the top face with the same velocity, thus conserving momentum in all directions, which is inconsistent with an infinite system having a velocity profile given by Eq. (10). To model such a system, we force the molecule entering the box at the top face to have an x -component velocity consistent with the prevailing Gaussian velocity profile given by Eq. (10). Since the image molecule is farther from the center of the Gaussian profile than the central molecule the instant it enters the box, it is given a slightly smaller x -component velocity according to Eq. (10). During the

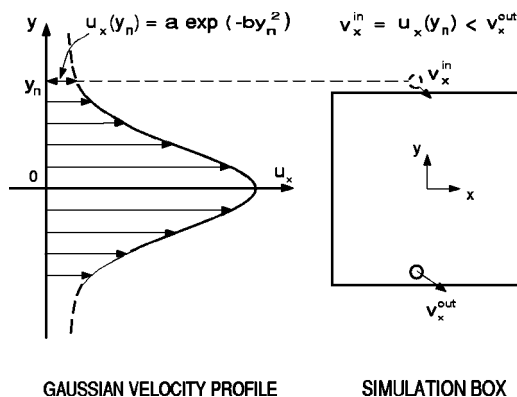


FIG. 1. Schematic diagram showing the modification of the periodic boundary condition in the y direction in a two-dimensional simulation box.

course of the simulation, this modification to the x -component velocity gives rise to the desired momentum loss through these two faces. To recap, whenever a molecule leaves the box through one of the x - z faces, the x velocity of the mirror molecule is replaced by the extrapolated value of the Gaussian velocity profile at the y coordinate of the mirror molecule at the time step before it enters the box. The other two components of the velocity are left unchanged.

To determine this extrapolated value of the Gaussian velocity (say, at time t), we need to know the Gaussian velocity profile at this time. In other words, we require the peak height, $u_p(t)$, and the variance, $\sigma^2(t)$, of the Gaussian velocity profile. For this purpose, the range from $y = -L/2$ to $y = L/2$ is divided into N_b bins, each of width $\Delta = L/N_b$, and having midpoints y_m , where $m = 1, 2, \dots, N_b$. The basic information recorded is the average x -component velocity of molecules in each of those bins, denoted as v_m . The number of bins N_b should be sufficiently large (about 20) to obtain a satisfactory resolution of the Gaussian. Also, the bins should have a sufficient number of molecules (about 100) to produce a well-defined drift velocity in each bin. At each time step the average velocity in each bin, v_m , is calculated and the resulting velocity profile is fitted to the two-parameter Gaussian function given by

$$u_x(t) = u_p(t) e^{-y^2/\sigma^2(t)}. \quad (14)$$

The two fit parameters, $u_p(t)$ and $\sigma^2(t)$, are then used to determine the extrapolated x -component velocity, $u_x^E(t)$, of the image molecule entering the box to replace a molecule leaving the box through the x - z faces, given by

$$u_x^E(t) = u_p(t) e^{-y^2(t-\Delta t)/\sigma^2(t)}, \quad (15)$$

where $y(t-\Delta t)$ is the y coordinate of the image molecule at the time step before it enters the box. The same fit parameters are used to determine the peak velocity at each time step, which is then plotted as a function of time to obtain the shear viscosity from Eq. (13). Hence, at no time do we require the value of shear viscosity to extrapolate the velocity profile, as the shear viscosity is manifested in the self-similar decaying nature of the imposed Gaussian velocity profile given by Eq. (10). An obvious advantage of this method is that we do not calculate the stress tensor, which is notori-

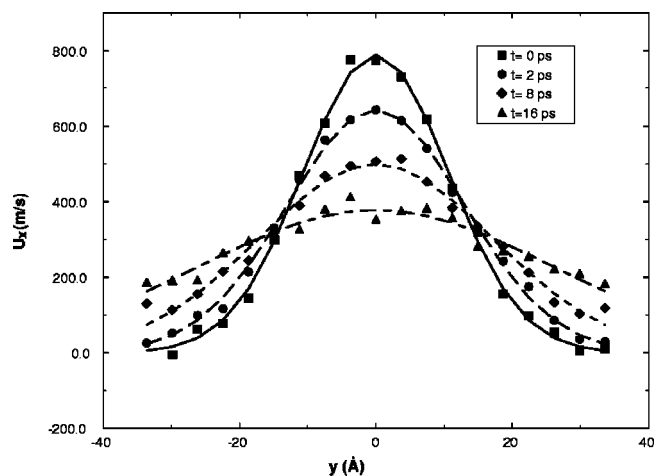


FIG. 2. The decay of the Gaussian velocity profile observed during the course of a simulation of argon with initial parameters $a_0=787 \text{ ms}^{-1}$ and $b_0=4.3 \times 10^{17} \text{ ms}^{-1}$. The velocity profile is recorded at the instants $t = 0, 2, 8,$ and 16 ps , shown as distinct points. The least-square fits are plotted along each profile as shown by continuous curves.

ously difficult to compute and fluctuates very rapidly, as in the case of EMD and NEMD methods. Instead, we evaluate a less fluctuating and easily computed quantity, the average velocity in each bin. Figure 2 shows the evolution of the decaying Gaussian profile with time for the case of argon with initial parameters of $a_0=787 \text{ ms}^{-1}$ and $b_0=4.3 \times 10^{17} \text{ m}^{-2}$ using the modified periodic boundary conditions.

There are two main limitations of the current method, both of which stem from the nature of the periodicity imposed on the system. First, as with traditional EMD and NEMD methods, localized acoustic (phonon) fluctuations can travel back to the central box domain via PBC and amplify fluctuations within the box. The current method generates additional phonon waves due to the modification of velocities that takes place at the system boundaries. The artificial effects of these anomalous fluctuations are typically overcome through extrapolation of results using progressively larger simulation boxes. In the current approach, the phonon wave generated at $t=0$ will not return until $t_{\text{ph}}=L/c$, where c is the speed of sound in the medium. The Gaussian peak will remain uncorrupted by this effect for $t < t_{\text{ph}}$, or roughly the time it takes for $\sigma(t)/\sigma(0)$, the ratio of the Gaussian velocity width at time t to the initial width, to equal the characteristic length $\phi=4\nu L/c$, where ϕ is determined by the competition between diffusive spreading of momentum and acoustic speed. The present method is thus viable if the viscosity can be estimated during the short-time decay $t < t_{\text{ph}}$. For $t > t_{\text{ph}}$, the momentum impulse starts to interact with the phonons and the viscosity cannot be reliably computed. The second limitation results from the modified PBC. The actual velocity profile is only pseudoinfinite. A molecule inside the central simulation box but near the x - z face “feels” a fluid structure and flow field consistent with a decaying Gaussian velocity profile in the direction towards the center of the box. However, in the direction away from the center of the box, it feels a periodic image consistent with traditional PBC (see Fig. 1). That is, the instantaneous positions and velocities of molecules in the image boxes are

consistent with traditional PBC, while the infinite decaying velocity profile is only mimicked in the central box whenever molecules cross the x - z faces. Molecules near the center of the main box, where the Gaussian peak height is recorded, do not feel these edge effects until they propagate from the edges in a time roughly equal to t_{ph} . Thus, the current method should be applicable for those systems in which the viscosity can accurately be computed in times less than t_{ph} . Both these effects can be minimized by choosing a small or localized initial Gaussian velocity profile which decays slowly near the boundaries.

From the above discussion it is clear that the determination of the correct size and shape of the initial Gaussian impulse, governed by the parameters a_0 and b_0 , respectively, is crucial. The value of b_0 can be fixed based on the fact that a localized Gaussian which is very flat near the boundaries is required to avoid the boundary effects discussed before. A localized Gaussian profile also is easier to fit and gives a smoother peak velocity. This means that the “hump” in the initial Gaussian profile should be well within the box. Characterizing the length scale of the hump as $2\sigma(0)$ ($=2b_0^{-1/2}$), we require that

$$b_0 \gg 4/L^2, \quad (16)$$

thus fixing the lower bound on b_0 . A good estimate for the value of b_0 would be $\sim 5 \times 4/L^2$. To get a well-defined drift velocity, the macroscopic drift velocity should be larger than the thermal fluctuations in a bin. These fluctuations in the x direction are of the order of $(k_B T/mN)^{1/2}$, where m is the mass of the molecule, and N is the number of molecules in the bin. Therefore, to observe an appreciably well-resolved Gaussian signal, we require

$$a_0 \gg (k_B T/mN)^{1/2}. \quad (17)$$

Excessively large values of a_0 produce large velocity gradients (i.e., shear rates) in the box, resulting in shear thinning.¹³ Thus, there exists an upper limit to the value of a_0 which can be realized by writing down the expression for the average shear rate of the initial Gaussian velocity profile given by

$$\dot{\gamma}_{\text{avg}} = 2a_0[1 - \exp(-b_0 L^2/4)]/L. \quad (18)$$

The exponential term is negligible for the values of b_0 chosen, and therefore $\dot{\gamma}_{\text{avg}} \approx 2a_0/L$. Assuming that shear thinning starts to occur for shear rates greater than $\dot{\gamma}_{\text{max}}$, we require $\dot{\gamma}_{\text{avg}} < \dot{\gamma}_{\text{max}}$ for Newtonian behavior to prevail. Therefore, a_0 should satisfy the condition

$$a_0 < \dot{\gamma}_{\text{max}} L/2. \quad (19)$$

The value of $\dot{\gamma}_{\text{max}}$ can be estimated as the inverse of the longest relaxation time of molecules τ , which can be estimated for linear molecules from the integral of the end-to-end vector autocorrelation function.¹⁴ The relaxation time is difficult to estimate for atomic species, but can be approximated as the time taken for the diffusion length to become equal to σ , i.e., $\tau \approx \sigma^2/6D_s$, where σ is the atomic diameter

TABLE I. Potential energy functions and parameters for the TraPPE united atom model used in this work for simulating butane.

	Potential energy function	Potential energy parameters
Nonbonded	$V_{\text{LJ}}=4\epsilon_{ij}[(\sigma_{ij}/r_{ij})^{12}-(\sigma_{ij}/r_{ij})^6]$	$\sigma_{\text{CH}_3}=3.77 \text{ \AA}$, $\epsilon_{\text{CH}_3}/k_B=98.1 \text{ K}$ $\sigma_{\text{CH}_2}=3.93 \text{ \AA}$, $\epsilon_{\text{CH}_2}/k_B=47.0 \text{ K}$ $k_b/\tilde{k}_B=452\,900 \text{ K \AA}^{-2}$ $r_0=1.54 \text{ \AA}$
Bond stretching	$V_b=(1/2)k_b(r-r_0)^2$	$k_\theta/k_B=62\,500 \text{ K rad}^{-2}$ $\theta_0=114^\circ$
Bond-angle bending	$V_\theta=(1/2)k_\theta(\theta-\theta_0)^2$	$a_0/k_B=0.0 \text{ K}$ $a_1/k_B=355.03 \text{ K}$ $a_2/k_B=-68.19 \text{ K}$ $a_3/k_B=791.32 \text{ K}$
Torsion	$V_\phi=a_0+a_1(1+\cos\phi)$ $+a_2(1-\cos 2\phi)$ $+a_3(1+\cos 3\phi)$	

and D_s is the self-diffusivity. Thus, $\dot{\gamma}_{\text{max}}$ can be quickly determined from a short EMD simulation of the species under concern.

For the rest of this paper, we will refer to the proposed algorithm as the momentum impulse relaxation (MIR) method. The MIR method is essentially a zero wave vector technique in the sense that it mimics a pseudoinfinite system. By using a highly localized Gaussian velocity profile with modification of velocities at the boundaries, phonon feedback due to periodicity is minimized. This effectively eliminates the dependence of shear viscosity on the wave vector. We note that the local shear rate, which is related to the slope of the Gaussian velocity profile, varies along the length of the simulation box and with time. Since the shear viscosity is dependent on the shear rate above the critical shear rate $\dot{\gamma}_{\text{max}}$, the viscosity computed using the MIR method at high shear rate is a convolution of many local shear rate-dependent viscosities. To eliminate this complication, as discussed before, a small Gaussian profile is used where the local shear rate along the box at all times is less than $\dot{\gamma}_{\text{max}}$. This enables accurate calculation of the shear rate-independent Newtonian viscosity.

IV. SIMULATION DETAILS

A. Argon

The shear viscosity of liquid argon at a density of 1.42 gcm^{-3} , temperature of 143.4 K , and pressure of 23.7 MPa (pressure obtained from an EMD simulation, which includes long-range pressure correction) is obtained using the MIR method and compared with those obtained by standard EMD and NEMD techniques. For the MIR method, we use a simulation box of dimensions $L/2 \times L \times L/2$, where L is the length of the box in the y direction and is equal to 71 \AA . The box contains 2000 argon atoms treated as Lennard-Jones (LJ) spheres with parameters $\epsilon/k_B=119.8 \text{ K}$ and $\sigma=3.41 \text{ \AA}$. The LJ potential is cut off at a radius of 3σ . Newton's equations of motion for these molecules are integrated using the velocity Verlet algorithm² with a time step of 2.17 fs . The system is equilibrated for 20 ps using EMD with standard PBC and velocity scaling. The Gaussian velocity profile is then introduced in the equilibrated system at time $t=0$ with the parameters $a_0=77 \text{ ms}^{-1}$ and $b_0=4.30 \times 10^{17} \text{ m}^{-2}$. The length of the box in the y direction is divided into 19 bins, each of

width 3.74 \AA . The peak velocity is determined from a least-square fit to the average drift velocities calculated in each bin at every time step. To investigate the non-Newtonian decay of this peak, we repeat the above procedure for larger values of a_0 as discussed in the next section. All argon simulations reported here are performed in the canonical ensemble, where the temperature is kept constant using a Nosé–Hoover thermostat¹⁵ with a time constant of 0.054 ps . Each of these simulations is run for a time of 10 ps .

The NEMD and EMD simulations are performed in a cubic simulation box of edge length 36 \AA containing 1000 atoms. For NEMD runs (for both argon and n -butane) we use the Sllod algorithm along with ‘‘sliding brick’’ boundary conditions. The NEMD simulation runs vary from 0.2 ns for the largest shear rate to 1 ns , for the smallest shear rate. The EMD run consists of one long run of approximately 1 ns . The rest of the parameters remain the same as those used for the MIR method.

B. Butane

Liquid n -butane is simulated at a density of 0.583 gcm^{-3} , a temperature of 291.5 K , and a pressure of 2.07 MPa (obtained from an EMD simulation). A simulation box of the same shape as that used for argon is chosen (with L being equal to 87.2 \AA) to simulate the above system using the MIR method. The simulation box contains 1000 butane molecules which are represented using a united atom (UA) model in which the hydrogen atoms are incorporated within the CH_3 and CH_2 groups. The force field used here is a version of the transferable potentials for phase equilibrium (TraPPE) model proposed by Sieppman and co-workers.^{16,17} The potential energy functions and the parameters used in this model are presented in Table I. The model accounts for bond stretching, bond bending, torsional rotations and van der Waals interactions. The intermolecular interactions are given by a Lennard–Jones potential with a cutoff of 10 \AA . For interactions between different groups a geometric combining rule is used, so that $\sigma_{ij}=(\sigma_{ii}\sigma_{jj})^{1/2}$ and $\epsilon=(\epsilon_{ii}\epsilon_{jj})^{1/2}$. Bond stretching and bond angle bending potentials are described with harmonic functions. A commonly used dihedral angle potential function proposed by Jorgensen and co-workers¹⁸ is also used. Long-ranged corrections are included in the calculation of pressure. A multiple time step algorithm is used to integrate the equations of motion with a

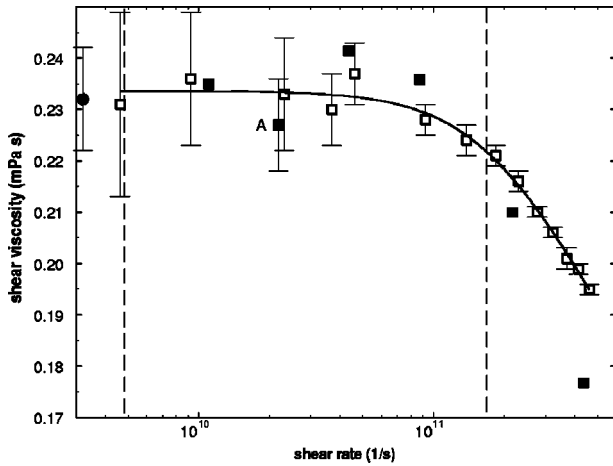


FIG. 3. Shear viscosity (η) versus shear rate ($\dot{\gamma}$) for argon. The open squares with error bars represent the NEMD simulation results. The solid line is the Carreau fit for the NEMD data. The filled squares are the shear viscosities obtained for different average shear rates of the Gaussian velocity profile at time $t=0$ using the MIR method. The filled square with error bars, labeled “A,” refers to the shear viscosity at $a_0=77 \text{ ms}^{-1}$, which has been used for comparison with EMD and NEMD methods. The solid circle with error bars represents the viscosity obtained from EMD. The two vertical dotted lines show the average shear rates corresponding to the upper and lower bounds on the value of a_0 .

time step of 1 fs for the fast modes and a large time step of 4 fs for the slower modes. The temperature is kept constant using a Nosé–Hoover thermostat with a time constant of 0.1 ps. The details on the equations of motion, the multiple time step algorithm and the thermostat are given elsewhere.¹⁴ The system is equilibrated for 10 ps before the Gaussian x velocity with parameters $a_0=90 \text{ ms}^{-1}$ and $b_0=5.0 \times 10^{17} \text{ m}^{-2}$ is imposed. The box is again divided into 19 bins along the y length of the box. The average velocities in these bins are least-square fitted to a Gaussian function every time step. The peak velocity data are collected every time step as before. The shear thinning behavior is also investigated in this case by repeating the above procedure for larger values of a_0 (i.e., larger shear rates).

The NEMD and EMD runs for n -butane are performed in a cubic simulation box of edge length 34.6 \AA containing 250 molecules. The force field, the multiple time step algorithm, and thermostat remain the same as used in the MIR method. The NEMD runs for the different shear rates vary from 0.4 ns for the largest shear rate to 1.6 ns for the smallest shear rate, whereas the EMD run consists of one long run of 1.6 ns.

V. RESULTS AND DISCUSSION

We begin by reporting the EMD, NEMD, and MIR results for shear viscosity of argon under the physical conditions specified earlier. The shear viscosity computed from EMD using the Green–Kubo expression is 0.232 mPa s . The atomic virial is used to calculate the three pressure terms, P_{xy} , P_{xz} , and P_{yz} at every time step and the shear viscosity is obtained by averaging over the three integrals [Eq. (1)].

We then conducted NEMD simulations to obtain the shear viscosity. Figure 3 shows the shear viscosity as a func-

TABLE II. Shear viscosity (η) values for argon and n -butane from NEMD simulations at different shear rates ($\dot{\gamma}$).

Argon			Butane		
$\log \dot{\gamma} (\text{s}^{-1})$	$\eta (\text{mPa s})$	$t_{\text{run}} (\text{ps})$	$\log \dot{\gamma} (\text{s}^{-1})$	$\eta (\text{mPa s})$	$t_{\text{run}} (\text{ps})$
9.66	0.231 ± 0.018	1000	10.70	0.129 ± 0.011	1600
9.96	0.236 ± 0.013	1000	11.00	0.130 ± 0.007	1600
10.36	0.233 ± 0.011	1000	11.30	0.129 ± 0.005	1000
10.57	0.230 ± 0.007	1000	11.60	0.125 ± 0.005	1000
10.66	0.237 ± 0.006	500	11.78	0.120 ± 0.003	1000
10.97	0.228 ± 0.003	500	11.90	0.116 ± 0.002	1000
11.14	0.224 ± 0.003	500	12.00	0.113 ± 0.001	400
11.27	0.221 ± 0.002	500	12.08	0.110 ± 0.002	400
11.36	0.216 ± 0.002	500	12.15	0.106 ± 0.001	400
11.44	0.210 ± 0.001	200	12.20	0.104 ± 0.002	400
11.51	0.206 ± 0.001	200	12.26	0.102 ± 0.001	400
11.56	0.201 ± 0.002	200	12.30	0.100 ± 0.001	400
11.62	0.199 ± 0.001	200			
11.66	0.195 ± 0.001	200			

tion of the shear rate computed from NEMD simulations; the results are also tabulated in Table II. The fluid exhibits non-Newtonian behavior (shear thinning) at high shear rates, with the plateau value at low shear rates giving the Newtonian viscosity. The solid line is the fit to the simulated values using the three-parameter Carreau model¹⁹

$$\eta = \frac{\eta_0}{(1 + (\lambda \dot{\gamma})^2)^\alpha}, \quad (20)$$

where η_0 is the Newtonian shear viscosity, and λ and α are the other two parameters. The Newtonian viscosity obtained from the NEMD simulations is 0.235 mPa s , which is nearly identical to that obtained using EMD. The Newtonian viscosity obtained by fitting the results to another model²⁰ is around 7% higher, and is not reported here.

Before presenting results from application of the MIR method to argon, we would like to confirm that the values of a_0 and b_0 chosen satisfy the requirements set by Eqs. (16), (17), and (19). First, the chosen value of b_0 is well above the lower limit of $4/L^2$ ($= 5.3 \times 10^{16} \text{ m}^{-2}$). The critical shear rate at which Newtonian behavior disappears is estimated to be $16.8 \times 10^{10} \text{ s}^{-1}$, this being calculated as the inverse of the relaxation time, τ , estimated from the self-diffusivity of argon. The value of a_0 associated with this value of $\dot{\gamma}_{\text{max}}$ is 594 ms^{-1} , which corresponds to its upper limit. The fluctuations in the x velocity in each bin are on the order of 17 ms^{-1} , which sets the lower limit for the a_0 . To obtain a good estimate of the Newtonian viscosity using the above criteria, we found the value of $a_0=77 \text{ ms}^{-1}$ to be the most appropriate. The fluctuations are significant compared to the drift velocity, especially near the box boundaries where the drift velocity is small. Therefore, we ran 20 similar runs, each starting from a different initial configuration of molecules, and the results presented here are the averages over these 20 runs. Figure 4 shows the observed decay of the peak velocity with time. The decays corresponding to the shear viscosity obtained from the EMD and NEMD methods are also plotted in the same figure for comparison. We can observe qualitatively that the viscosity obtained from the MIR

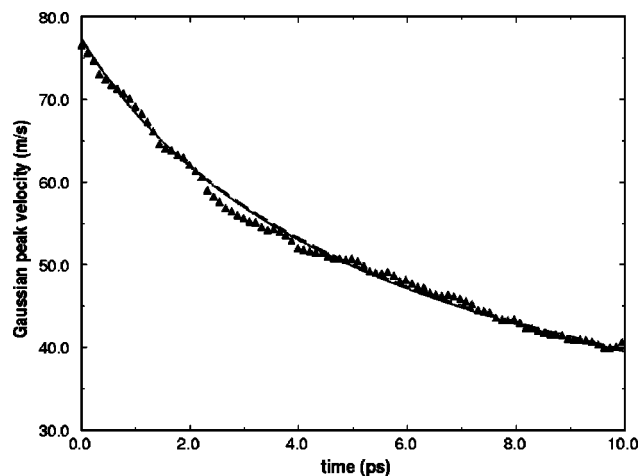


FIG. 4. Decay of the Gaussian peak velocity with time for argon with $a_0 = 77 \text{ ms}^{-1}$ and $b_0 = 4.3 \times 10^{17} \text{ m}^{-2}$. The triangles represent the actual decay obtained from our simulations. The solid curve refers to the decay corresponding to viscosity obtained from NEMD simulations. The dashed curve refers to the decay corresponding to viscosity obtained from EMD simulations.

method matches very well with those obtained from NEMD and EMD. The value of the shear velocity obtained is equal to 0.227 mPa s . This value of viscosity is 3% lower than that obtained from NEMD and 2% lower than that obtained from EMD simulations. These differences are well within the statistical errors of the simulations, as well as within the error associated with the fitting procedures used to extrapolate NEMD results to the Newtonian viscosity. The statistical uncertainty of this viscosity value is estimated by dividing these 20 runs into 3 blocks containing nearly equal number of runs, calculating the standard deviation of the average viscosities in each block, and then dividing this value by 3. The statistical uncertainty is nearly of the same magnitude as the uncertainties obtained from the EMD and NEMD runs, as shown in Fig. 3. Thus, the MIR method gives Newtonian viscosities that are identical to those obtained from EMD and NEMD. We notice that during the simulation length ($=10 \text{ ps}$) no boundary effects or phonon modes are observed in our simulations, indicating that the Gaussian fit is good for $t < t_{\text{ph}}$ (where c for argon in these conditions is $\sim 500 \text{ ms}^{-1}$, therefore $t_{\text{ph}} \sim 14 \text{ ps}$), *viz.*, L is sufficiently large that the

spreading profile does not “see” the box boundary through phonon interaction and remains a Gaussian.

To determine the degree of shear thinning that occurs at the chosen value of a_0 , the shear rate is estimated as the average shear rate along the length of the simulation box at time $t=0$ at these values of a_0 and b_0 using Eq. (18). For the a_0 and b_0 used here, $\dot{\gamma}_{\text{avg}}$ is equal to $2.17 \times 10^{10} \text{ s}^{-1}$, which corresponds to point A in Fig. 3. We can see that at this small shear rate, the shear thinning is minimal and the observed viscosity is very close to the Newtonian viscosity. Shear thinning can be observed if larger values of the parameter a_0 are used. In Fig. 3, calculated viscosities obtained are plotted as a function of the *initial* average shear rate corresponding to each value of a_0 . We can clearly see that as a_0 increases (or, as the average shear rate increases), the viscosity drops, thereby confirming that shear thinning does occur at large values of a_0 . The results are also presented in detail in Table III. It should be emphasized that this is just a crude way of showing non-Newtonian behavior, since the shear viscosity varies across the length of the simulation box and also varies with time (viscosity is dependent on the shear rate, which itself varies with time and position along the y direction). Also shown in Fig. 3 as dashed lines are the shear rates corresponding to the upper and lower limits on a_0 . We also conducted a series of simulation runs at a very small value of a_0 ($=40 \text{ ms}^{-1}$) to verify the accuracy of the shear viscosity reported earlier (using the MIR method). The shear viscosity obtained is plotted as the filled square to the left of point A in Fig. 3, and it can be observed that the value agrees very well with the shear viscosity reported earlier (point A). Lower values of a_0 were also tried, but the signal-to-noise ratio was too low to obtain reliable results.

We now present the results for *n*-butane in the same order as presented for the case of argon. The shear viscosity obtained from the EMD technique using the Green–Kubo expression is equal to 0.135 mPa s . We ran the simulation for approximately 1.6 ns , therefore resulting in an uncertainty of approximately 5% using Eq. (3). Figure 5 shows the shear viscosity as a function of the shear rate obtained from the NEMD runs. These results are also presented in Table II. The solid line is the fit to the simulated values using the Carreau model given by Eq. (20). We obtained a shear viscosity of

TABLE III. The MIR results: Shear viscosity (η), average initial shear rate ($\dot{\gamma}_{\text{avg}}$) and number of runs (N_{run}) for different values of a_0 . The statistical uncertainties (not reported for all values of a_0) in the tabulated shear viscosities decrease as larger values of a_0 are used. N_{runs} refers to the number of simulation runs conducted and averaged over to obtain the shear viscosity.

Argon				Butane			
a_0 (ms^{-1})	$\log \dot{\gamma}_{\text{avg}}$ (s^{-1})	η (mPa s)	N_{runs}	a_0 (ms^{-1})	$\log \dot{\gamma}_{\text{avg}}$ (s^{-1})	η (mPa s)	N_{runs}
39	10.037	0.235	40	90	10.316	0.1320 ± 0.01	20
77	10.338	0.227 ± 0.009	20	200	10.663	0.1323	20
154	10.639	0.241	10	500	11.061	0.1320	10
308	10.940	0.238	5	1000	11.360	0.1288	5
770	11.338	0.210	3	2000	11.662	0.1125	5
1540	11.639	0.177	2				

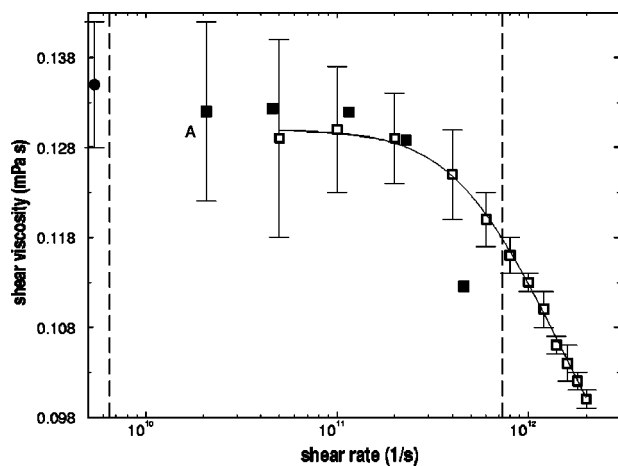


FIG. 5. Shear viscosity (η) versus shear rate ($\dot{\gamma}$) for butane. The open squares with error bars represent the NEMD simulation results. The solid line is the Carreau fit for the NEMD data. The filled squares are the shear viscosities obtained for different average shear rates of the Gaussian velocity profile at time $t=0$. The filled square with error bars, labeled “A,” refers to the shear viscosity at $a_0=90 \text{ ms}^{-1}$ which has been used for comparison with EMD and NEMD methods. The solid circle with error bars represents the viscosity obtained from EMD. The two vertical dotted lines show the average shear rates corresponding to the upper and lower bounds on the value of a_0 .

0.130 mPa s from the fit, in good agreement with EMD results.

A similar analysis as before is done to obtain estimates of the upper and lower bounds of the MIR velocity profile parameters. The lower bound on the value of b_0 is $5.3 \times 10^{16} \text{ m}^{-2}$ as calculated from Eq. (16), which is well below the value of $5 \times 10^{17} \text{ m}^{-2}$ chosen here. The longest relaxation time in butane is 1.37 ps, which is the rotational relaxation time calculated from an EMD simulation. Therefore, $\dot{\gamma}_{\text{max}} = 7.3 \times 10^{11} \text{ s}^{-1}$, which corresponds to the upper bound value of 3140 ms^{-1} for a_0 . The lower bound for a_0 is 28 ms^{-1} , corresponding to the thermal fluctuations. Again, the chosen value of a_0 ($=90 \text{ ms}^{-1}$) to obtain the Newtonian viscosity is found to be very appropriate. Twenty simulations starting from different initial configurations were conducted and averaged to improve the signal-to-noise ratio. Figure 6 shows the average decay of the peak velocity for the 20 runs. The value of shear viscosity obtained from the MIR method is equal to 0.132 mPa s, which is about 2% higher than those obtained from EMD and NEMD simulations. Again, these results are within the statistical accuracy of the EMD and NEMD results, indicating that the MIR method yields identical viscosities. No boundary effects are noticed as the simulation length $t=10 \text{ ps}$ is about the same as $t_{\text{ph}}=8.5 \text{ ps}$ (with $c \sim 950 \text{ ms}^{-1}$). Point A in Fig. 5 corresponds to the average shear rate at the beginning of the run at the viscosity just obtained. We can again see that at this low shear rate, shear thinning is negligible and the observed viscosity is very close to the Newtonian viscosity. A similar analysis, as in the case of argon, is done to obtain the approximate shear rate dependence of the viscosity. The viscosities obtained for larger values of a_0 from the MIR method are plotted as a function of the average shear rates in Fig. 5. The results are tabulated

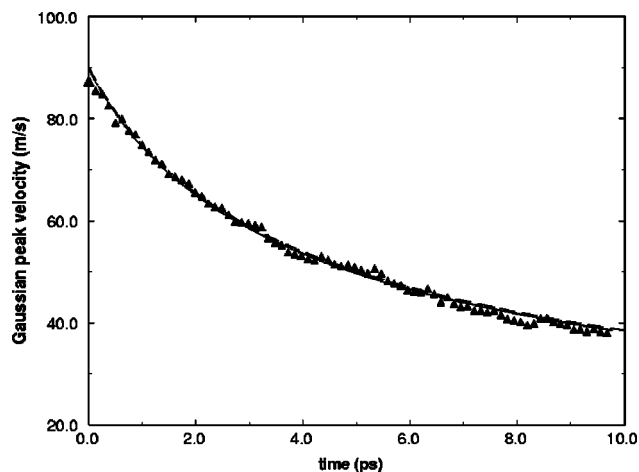


FIG. 6. Decay of the Gaussian peak velocity with time for *n*-butane with $a_0=90 \text{ ms}^{-1}$ and $b_0=5.0 \times 10^{17} \text{ m}^{-2}$. The triangles represent the actual decay obtained from our simulations. The solid curve refers to the decay corresponding to viscosity obtained from NEMD simulations. The dashed curve refers to the decay corresponding to viscosity obtained from EMD simulations.

in Table III. The upper and lower bounds on the values of a_0 are shown in the same figure as dashed, vertical lines.

The main advantage of the MIR method for calculating shear viscosity of fluids is that the lengths of the simulations are significantly shorter than those corresponding to the EMD or NEMD methods (by a factor of ~ 100). Although a larger simulation box is required to eliminate edge effects and obtain a well-resolved Gaussian profile, the computational savings are still on the order of 20–30 times. It is worth mentioning that large system sizes are typically not the biggest problem in MD, since parallelization strategies such as domain decomposition become more effective for larger systems. What makes EMD and NEMD methods so computationally demanding is the long simulation times that are required, particularly for computing collective transport properties such as viscosity. The MIR method is desirable in this regard, because although it requires large system sizes, fairly short simulation lengths are required, making it an easily parallelizable technique. In this work we have not tried to investigate if accurate shear viscosities can be obtained with systems smaller than those used in this work. Reducing the system size would lead to highly fluctuating drift velocities in the bins, and hence a very noisy Gaussian peak velocity. This means that large values of a_0 would have to be used, which leads to shear thinning. On the other hand, the use of a larger system would enable us to use small values of a_0 , and hence obtain more accurate estimates of the Newtonian shear viscosity, but the CPU time would be longer.

Table IV summarizes the computational advantages of using the method proposed here over conventional EMD and NEMD methods. We have only used simple “independent run” parallel computation for the 20 runs required by our methodology and the multiple runs required for NEMD at different shear rates. Therefore, the wall clock times required by the MIR method are smaller by a factor of 20 than the total CPU times required. This is not true for the NEMD simulations, as the runs are not equal in length. Therefore,

TABLE IV. Comparison of the EMD, NEMD, and MIR methods of obtaining Newtonian shear viscosity in terms of the computational requirements, system sizes, and simulation lengths.

	Argon			Butane		
	EMD	NEMD	MIR	EMD	NEMD	MIR
No. of molecules/atoms	1000	1000	2000	250	250	1000
No. of runs	1	14	20	1	12	20
Simulation length ^a (ps)	1000	1000	10	1600	1600	10
Total CPU time ^b (hrs)	21	170	12	19	125	25
Wall clock time ^c (hrs)	21	23	0.6	19	22	1.3

^aThe longest of the multiple NEMD runs is tabulated.

^bAll simulations performed on SunSPARC ULTRA 5 workstations. The total CPU time being calculated as the sum of the individual CPU times of each run in case of multiple runs.

^cThe wall clock time of the NEMD run is greater than that of an EMD run for the same system size and simulation length because the neighbor list used is not as efficient for NEMD as it is for EMD.

the wall clock time required is limited by the longest run, invariably the run at the lowest shear rate. It should be emphasized that the purpose of this paper is not to compare the EMD and NEMD methods, and that a more exhaustive comparison might yield slightly different performance results for these methods. What the present analysis shows is that the MIR method results in a significant reduction in computational time over the EMD and NEMD methods while yielding a high degree of accuracy.

VI. CONCLUSIONS

In this paper, a novel momentum impulse relaxation method for determining the shear viscosity of Newtonian liquids has been introduced. The method is based on the fact that a parallel Gaussian flow in an infinite domain, if left unperturbed, decays with time in a self-similar manner. In particular, the decay of the peak of the Gaussian velocity profile is directly related to viscosity of the fluid as shown theoretically in Sec II. This idea has been incorporated into a molecular dynamics simulation algorithm, which involves modifying the periodic boundary conditions in the direction of momentum transfer so as to enable momentum to diffuse out and give the correct transient behavior of the velocity profile. A localized Gaussian velocity profile is used which minimizes phonon corruption due to periodicity. Physical criteria have also been presented to enable a user to choose the ideal Gaussian velocity profile which would give accurate estimates for the Newtonian shear viscosity. The proposed methodology has been used to determine the Newtonian shear viscosity for a system of argon atoms and *n*-butane molecules. The shear viscosities obtained from the short-time decay of the peak velocity in our method are within 2%–3% of the values obtained from the EMD and NEMD methods, which are well within the uncertainties of the EMD and NEMD simulations. The main advantage of this method is that it is very computationally efficient and accurate values of viscosity can be obtained with huge reductions in the computational time, on the order of 20–30 times, even though larger systems have to be used.

In the future, we would like to apply this methodology to more viscous systems such as polymers and long hydrocar-

bons, where current EMD and NEMD methods require prohibitively large times to determine the shear viscosity. Since these molecules have high viscosities the Gaussian velocity profile in our methodology would decay quite rapidly, thus requiring very short simulation lengths. Though these molecules would shear thin at very small shear rates, the thermal fluctuations would also be much smaller, allowing us to simulate in the small shear rate regions, i.e., small values of a_0 .

ACKNOWLEDGMENTS

We acknowledge financial support from the Mobil Foundation. Computational resources were provided by a grant from the Army Research Office (No. DAAG55-981-0091). E.J.M. wishes to acknowledge support from the National Science Foundation CAREER program (No. CTS-9701470). H.C.C. would like to acknowledge support from the Bayer chair fund. We would also like to thank Loukas I. Kioupis for several helpful discussions.

- ¹P. T. Cummings and D. J. Evans, *Ind. Eng. Chem. Res.* **31**, 1237 (1992).
- ²M. P. Allen and D. J. Tildesley, *Computer Simulations of Liquids* (Clarendon, Oxford, 1987).
- ³J. J. Erpenbeck, *Phys. Rev. A* **38**, 6255 (1988).
- ⁴B. L. Holian and D. J. Evans, *J. Chem. Phys.* **78**, 5147 (1983).
- ⁵B. J. Alder and T. E. Wainwright, *Phys. Rev. A* **1**, 18 (1970).
- ⁶M. Mondello and G. S. Grest, *J. Chem. Phys.* **106**, 9327 (1997).
- ⁷D. J. Evans and G. P. Morris, *Statistical Mechanics of Nonequilibrium Liquids* (Academic, London, 1990).
- ⁸E. M. Gosling, I. R. McDonald, and K. Singer, *Mol. Phys.* **26**, 1475 (1973).
- ⁹A. J. C. Ladd, *Mol. Phys.* **53**, 459 (1984).
- ¹⁰A. W. Lees and S. F. Edwards, *J. Phys. C* **5**, 1921 (1972).
- ¹¹J. Petracic and D. J. Evans, *Mol. Phys.* **95**, 219 (1998).
- ¹²J. Petracic and D. J. Evans, *Phys. Rev. E* **58**, 2624 (1998).
- ¹³S. Chynoweth, R. C. Coy, and Y. Michopoulos, *Proc. Inst. Mech. Eng., Part J* **209**, 243 (1995).
- ¹⁴L. I. Kioupis and E. J. Maginn, *Chem. Eng. J.* **74**, 129 (1999).
- ¹⁵S. Nosé, *Prog. Theor. Phys. Suppl.* **103**, 1 (1991).
- ¹⁶J. I. Siepmann, M. G. Martin, C. J. Mundy, and M. L. Klein, *Mol. Phys.* **90**, 687 (1997).
- ¹⁷M. G. Martin and J. I. Siepmann, *J. Phys. Chem. B* **102**, 2569 (1998).
- ¹⁸W. L. Jorgensen, J. D. Madura, and C. J. Swenson, *J. Am. Chem. Soc.* **106**, 6638 (1984).
- ¹⁹J. M. Dealy and K. S. Wissbrun, *Melt Rheology and its Role in Plastics Processing* (Van Nostrand Reinhold, New York, 1990).
- ²⁰S. H. Lee and P. T. Cummings, *J. Chem. Phys.* **99**, 3919 (1993).